Available online at http://ijim.srbiau.ac.ir/
Int. J. Industrial Mathematics (ISSN 2008-5621)
Vol. 8, No. 3, 2016 Article ID IJIM-00737, 14 pages
Research Article

Two-phase Boundary Layer Flow, Heat and Mass Transfer of a Dusty Liquid past a Stretching Sheet with Thermal Radiation

K. L. Krupa Lakshmi *, B. J. Gireesha †‡§, Rama S R Gorla ¶, B. Mahanthesh ‖

Received Date: 2015-08-11 Revised Date: 2016-01-06 Accepted Date: 2016-02-12

Abstract

The problem of two-phase MHD boundary layer flow, heat and mass transfer over a stretching sheet with fluid-particle suspension and thermal radiation has been studied. The effect of mass transfer in dusty fluid over a stretching sheet is considered for the first time. The governing equations are reduced to a set of non-linear ordinary differential equations under suitable similarity transformations. The transformed equations are then solved numerically. The influence of various physical parameters such as magnetic parameter, fluid-particle interaction parameters, Prandtl number, Eckert number and thermal radiation parameter on velocity, temperature and concentration of both fluid and particle phase is analyzed. The numerical results of the present investigation were compared with previously published results and found to be an excellent agreement. It is found that, the momentum, thermal and solute boundary layer thickness of both fluid and dust phase are reduced for higher values of mass concentration of suspended dust particles.

Keywords : Boundary layer flow; heat and mass transfer; Stretching sheet; Thermal radiation; Fluid-particle suspension; Numerical solution.

1 Introduction

The phenomenon of boundary layer flow, heat and mass transfer has many practical applications in industrial and manufacturing processes. The knowledge of heat and mass transfer within a thin liquid film is crucial in understanding the coating process, heat exchangers design and chemical processing equipments. Its relevance is also seen in polymer processing, wire and fibre coating, manufacturing of artificial films, food stuff processing and transpiration cooling. The major endeavour in almost every extrusion is to maintain the surface quality of the product. The problem of extrusion of thin surface layers needs special interest to gain some knowledge for controlling the coating efficiently. Therefore, a large number of researchers are actively engaged in this stream. The study of boundary layer flow over a stretched surface moving with a constant velocity was first initiated by Sakiadis [33]. He formulated the boundary layer equations for two dimensional symmetric flows. Tsou et al [34] analysed the effect of heat transfer on a con-

*Department of Studies and Research in Mathematics, Kuvempu University, Shimoga-577 451, Karnataka, INDIA.
†Corresponding author. bjgireesu@rediffmail.com
‡Department of Studies and Research in Mathematics, Kuvempu University, Shimoga-577 451, Karnataka, INDIA.
§Department of Mechanical Engineering, Cleveland State University, Cleveland, OHIO, USA.
¶Department of Mechanical Engineering, Cleveland State University, Cleveland, OHIO, USA.
‖Department of Mathematics and Statistics, Christ University, Bangalore-560027, Karnataka, INDIA.

tinuously moving surface with a constant velocity. Further, they validated the numerical results of [33] experimentally. Later on, heat and/or mass transfer over a stretched surface/channel with various aspects is carried out by many researchers ([18]-[12]).

It is worth to mention that, aforementioned investigations are concerned only with ordinary fluids. However, the fluid flow analysis embedded with dust particles is encountered in many engineering problems. In particular, this problem arises in a number of manufacturing processes such as nuclear reactors, waste water treatment, combustion, corrosive particles in engine oil flow, powder technology, rain erosion, paint spraying, soil erosion by natural winds, dust entrainment in a cloud during the nuclear explosion and etc. In view of this, Saffman [32] initiated to study on fluid-particle suspension and discussed the stability of laminar flow of a dusty gas. He made some assumptions on dust particles and formulated the equations of motion of dusty fluid. Later, Agranat [1] discussed the effect of pressure gradient on friction and heat transfer in a dusty fluid. The problem of compressible boundary-layer laminar flow of a particulate suspension over a semi-infinite flat plate was solved numerically by Chamkha [9]. Datta and Mishra [10] have investigated the boundary layer flow of a dusty fluid over a semi infinite flat plate. Vajravelu and Nayfeh [37] have studied hydromagnetic boundary layer flow of a dusty fluid over a stretching sheet with transpiration cooling. Heat transfer effects on dusty gas flow past a semi-infinite inclined plate was analysed by Palani and Ganesan [28]. Later on, Tiwari and Kamal [35] have studied the effect of Hall current on unsteady hydromagnetic boundary layer flow in rotating dusty fluid. An unsteady flow and heat transfer of dusty fluid between two parallel plates with variable viscosity and thermal conductivity has been investigated by Makinde and Chinyoka [24]. Recently, the problem of two-phase unsteady MHD Couette flow between two parallel infinite plates has been studied by Basant and Apere [5]. The porosity effect on the flow of a dusty fluid between parallel plates is studied by Attia et al [3]. Recently, the flow/heat transfer of dusty fluid with various aspects was examined by Gireesha et al ([13]-[17]).

In aforementioned dusty fluid problems; the mass transfer analysis is not considered. Thus, to fill this gap, an attempt has been made to analyse the mass transfer effects on two-phase boundary layer flow of dusty fluid over a stretching sheet. The effect of thermal radiation is also taken into account. The governing partial differential equations are transformed into a set of ordinary differential equations by introducing appropriate similarity transformations. These non-linear ordinary differential equations are then solved numerically using a shooting method along with fourth-fifth order Runge-Kutta-Fehlberg scheme. The effects of influential parameters in different flow fields are analyzed and discussed in detail with the help of graphs and tables.

2 Nomenclature

B_0 Magnetic field
b Positive constant
C_f Skin friction coefficient
C Concentration of the fluid
c Constant
c_m Specific heat coefficient of dust particles
c_p Specific heat
D_m The mass diffusivity coefficient
Ec Eckert number
f Dimensionless fluid phase velocity component
F Dimensionless dust phase velocity component
j_w Mass flux
K Stokes drag coefficient
k Thermal conductivity
k^+ Mean absorption coefficient
l Dust particle mass concentration parameter
M Magnetic parameter
m Mass of dust particle per unit volume
N Number density of dust particles
Nu_x Local Nusselt number
Pr Prandtl number
q_w Heat flux
q_r Radiative heat flux
R Thermal radiation parameter
r Radius of dust particles
Re_x Local Reynolds number
Sh Sherwood number
Sc Schmidt number
T Fluid phase temperature
u, v Fluid phase velocity components along x and y directions

u_w Stretching sheet velocity
x Coordinate along the plate
y Coordinate normal to the plate

Greek symbols

β_v Fluid-particle interaction parameter for velocity
β_c Fluid-particle interaction parameter for concentration
β_t Fluid-particle interaction parameter for temperature
μ Dynamic viscosity
σ Electric conductivity of the fluid
σ^* Stefan-Boltzmann constant
$\theta(\eta)$ Dimensionless fluid phase temperature
$\phi(\eta)$ Dimensionless fluid phase concentration
η Similarity variable
τ_T Thermal equilibrium time
τ_w Surface shear stress
τ_v Relaxation time of the dust particles
τ_c Solutal equilibrium time
γ Specific heat ratio
ρ Density of the base fluid

Superscript

$'$ Derivative with respect to η

Subscript

p Dust phase
w Fluid properties at the wall
∞ Fluid properties at ambient condition

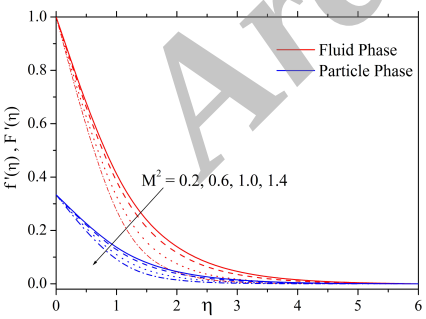

Figure 1: Influence of M^2 on velocity profile.

3 Description of the Problem

Consider a steady laminar two dimensional boundary layer flow of an incompressible electrically conducting dusty viscous fluid over a

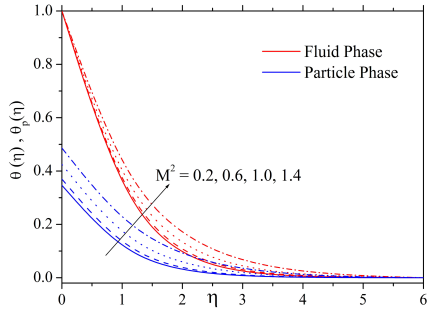

Figure 2: Influence of M^2 on temperature profile.

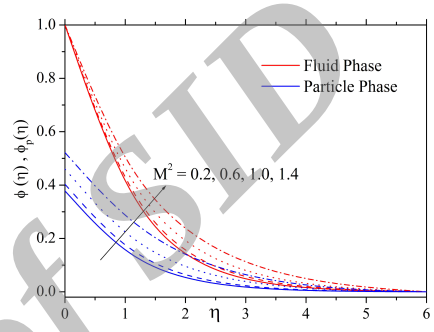

Figure 3: Influence of M^2 on concentration profile.

stretching sheet. The flow is assumed to be confined to the region of $y > 0$. The flow is generated by the action of two equal and opposite forces along the x-axis. A uniform magnetic field of strength B_0 is imposed along the Y-axis. The sheet is stretched with the linear velocity u_w along the X-axis. The dust particles are assumed to be spherical in shape and uniformly distributed throughout the fluid. The number density is assumed to be constant and volume fraction of dust particles is neglected. Besides, there is no radiative heat transfer from one particle to another. The fluid and dust particle motions are coupled only through drag, heat and mass transfer between them. The drag force is modelled using Stokes linear drag theory. Other interaction forces such as virtual force, shear lift force and spin-lift force will be neglected compared to the drag force [7]. The terms T_w and C_w represents the temperature and concentration of the fluid at the sheet respectively. Where as T_∞ and C_∞ are correspondingly denotes the ambient fluid temperature and concentration.

Under aforesaid assumptions with usual

Table 1: Comparison of the results for local Nusselt number $-\theta'(0)$ with $R = l = M = 0$.

Pr	Grubka et al [18]	Ishak [21]	El-Aziz [4]	Present Study
0.72	0.8086	0.8086	0.80873	0.808630
1.0	1.0000	1.0000	1.0000	1.0000
3.0	1.9237	1.9237	1.92368	1.92367
10.0	3.7207	3.7207	3.7207	3.72067
100	12.294	12.2941	12.2941	12.294087

Table 2: Numerical values of $f''(0)$, $-\theta'(0)$ and $-\phi'(0)$ for different values of $M^2, Ec, l, R, Sc, Pr, \beta_v, \beta_t$ and β_c.

M^2	Ec	l	R	Sc	Pr	β_v	β_t	β_c	$f''(0)$	$-\theta'(0)$	$-phi'(0)$
0	0.5	0.5	0.5	0.5	0.5	0.5	0.6	0.6	-1.08042	0.54830	0.70316
0.2									-1.09873	0.54605	0.69933
0.4									-1.15194	0.53965	0.68828
0.6									-1.23563	0.53573	0.67136
0.4	0	0.5	0.5	0.5	0.5	0.5	0.6	0.6	-1.23563	0.53573	0.67136
	0.2								-1.23563	0.53344	0.67136
	0.3								-1.23563	0.53229	0.67136
0.4	0.5	0	0.5	0.5	0.5	0.5	0.6	0.6	-1.07723	0.45616	0.62640
		0.5							-1.15194	0.53965	0.68828
		1.0							-1.22212	0.61018	0.74518
0.4	0.5	0.5	0	0.5	0.5	0.5	0.6	0.6	-1.15194	0.73285	0.68828
			1						-1.15194	0.44535	0.68828
			2						-1.15194	0.35196	0.68828
0.4	0.5	0.5	0.5	0	0.5	0.5	0.6	0.6	-1.15194	0.53965	0.16667
				0.5					-1.15194	0.53965	0.68828
				0.8					-1.15194	0.53965	0.93270
0.4	0.5	0.5	0.5	0.5	1	0.5	0.6	0.6	-1.15194	0.81848	0.68828
					3				-1.15194	1.56335	0.68828
					5				-1.15194	2.08068	0.68828
0.4	0.5	0.5	0.5	0.5	0.5	1	0.6	0.6	-1.18755	0.53504	0.68239
						1.5			-1.20841	0.53311	0.67913
						2			-1.22211	0.53217	0.67708
0.4	0.5	0.5	0.5	0.5	0.5	0.5	1	0.6	-1.15194	0.58859	0.68828
							1.5		-1.15194	0.63831	0.68828
							2		-1.15194	0.67960	0.68828
0.4	0.5	0.5	0.5	0.5	0.5	0.5	0.6	1	-1.15194	0.53965	0.70711
								1.5	-1.15194	0.53965	0.72107
								2	-1.15194	0.53965	0.73001

boundary layer approximations, the conservation of mass and momentum equations for both fluid and particle phase takes the following form [[9], [10] ,[3]];

$$\frac{\partial u}{\partial x} + \frac{\partial v}{\partial y} = 0, \quad (3.1)$$

$$\rho(u\frac{\partial u}{\partial x} + v\frac{\partial u}{\partial y}) = \mu\frac{\partial^2 u}{\partial y^2}$$

$$-\sigma B^2 u + KN(u_p - u), \quad (3.2)$$

$$\frac{\partial u_p}{\partial x} + \frac{\partial v_p}{\partial y} = 0, \quad (3.3)$$

$$\rho_p(u_p\frac{\partial u_p}{\partial x} + v_p\frac{\partial u_p}{\partial y}) = -KN(u_p - u), \quad (3.4)$$

where (u, v) and (u_p, v_p) denotes the velocity

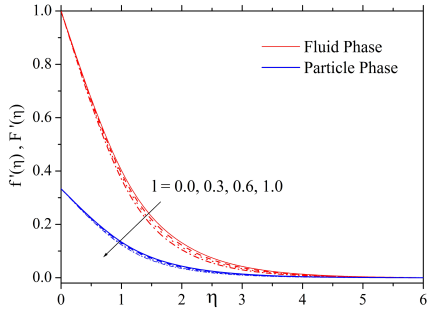

Figure 4: Influence of l on velocity profile.

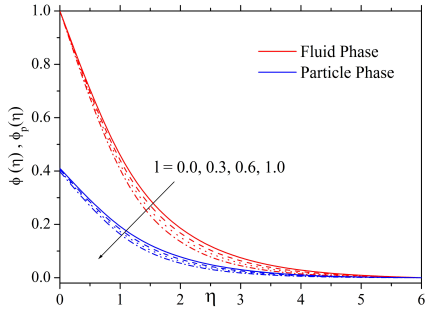

Figure 6: Influence of l on concentration profile.

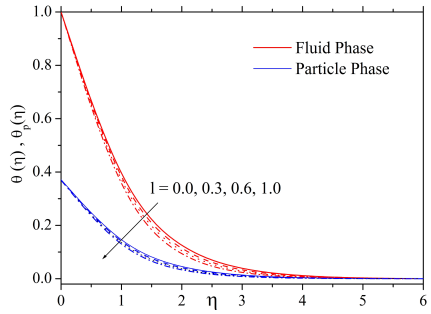

Figure 5: Influence of l on temperature profile.

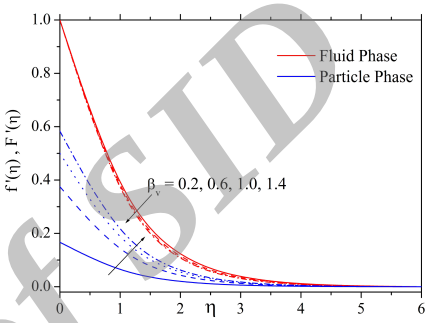

Figure 7: Influence of β_v on velocity profile.

components of the fluid and particle phase along the x and y directions respectively. ρ and ρ_p are density of the fluid and dust particles respectively. m -mass of dust particles per unit volume, N -number density of dust particles, σ-electrical conductivity of the fluid, μ-dynamic viscosity of the fluid, B_0-uniform magnetic field, $K = (6\pi\mu r)$ is the stokes drag coefficient [32] and r-radius of dust particle.

The last terms in the right hand side of equation (3.2) represents the force due to the relative motion between fluid and dust particles. Since the force exerted by the fluid on the dust particles is equal and opposite to that exerted by the dust particles on fluid; thus there must be an extra force term, equal in magnitude and opposite in sign, in the equation of motion for particles (see equation (3.4)).

The appropriate boundary conditions for the velocity are:

$$\begin{aligned} u = u_w(x), \;\; v = 0 \;\; \text{at} \;\; y = 0, \\ u \longrightarrow 0, \;\; u_p \longrightarrow 0, \\ v_p \longrightarrow v, \;\; \text{as} \;\; y \longrightarrow \infty, \end{aligned} \tag{3.5}$$

where $u_w(x) = bx$ is a stretching sheet velocity and $b > 0$ is stretching rate.

Equations (3.1) to (3.4) subjected to boundary condition (3.5), admits self-similar solution in terms of the similarity function f, F and the similarity variable η and they are defined as [see [37], [17]];

$$\begin{aligned} u = bxf'(\eta), \;\; v = -\sqrt{\nu b} f(\eta), \\ \eta = \sqrt{\frac{u_w}{\nu x}} y, \\ u_p = bxF'(\eta), \;\; v_p = -\sqrt{\nu b} F(\eta), \end{aligned} \tag{3.6}$$

where a prime denotes the differentiation with respect to η. In terms of relations (3.6), the equations (3.1) and (3.3)are identically satisfied, and the equations (3.2) and (3.4), will reduce into the following set of non-linear ordinary differential equations;

$$\begin{aligned} f'''(\eta) + f''(\eta) f(\eta) - f'(\eta)^2 \\ + l\beta_v \left[F'(\eta) - f'(\eta) \right] \\ - M^2 f'(\eta) = 0, \end{aligned} \tag{3.7}$$

$$\begin{aligned} F''(\eta) F(\eta) - F'(\eta)^2 \\ + \beta_v \left[f'(\eta) - F'(\eta) \right] = 0, \end{aligned} \tag{3.8}$$

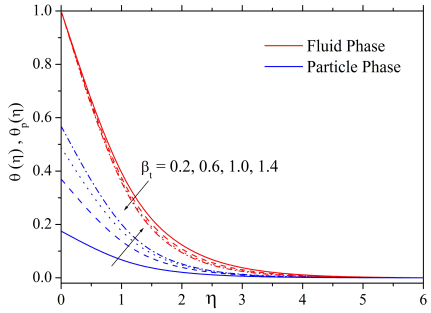

Figure 8: Influence of β_t on temperature profile.

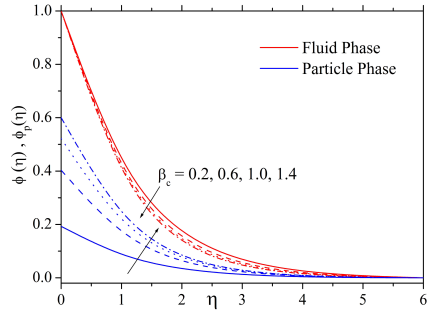

Figure 9: Influence of β_c on concentration profile.

Transformed boundary conditions are;

$$\begin{aligned} f'(\eta) = 1, \quad f(\eta) = 0 \text{ at } \quad \eta = 0, \\ f'(\eta) \longrightarrow 0, \quad F'(\eta) \longrightarrow 0, \\ F(\eta) \longrightarrow f(\eta) \text{ as } \eta \longrightarrow \infty, \end{aligned} \tag{3.9}$$

where $l = \frac{mN}{\rho}$ is the dust particles mass concentration parameter, $\tau_v = m/K$ is relaxation time of the dust particles i.e, the time required by a dust particle to adjust its velocity relative to the fluid, $\beta_v = \frac{1}{b\tau_v}$ is fluid-particle interaction parameter and $M^2 = \frac{\sigma B_0^2}{b\rho}$ is the magnetic parameter.

Heat Transfer Analysis

The governing boundary layer heat transport equations for both fluid and dust phase are given

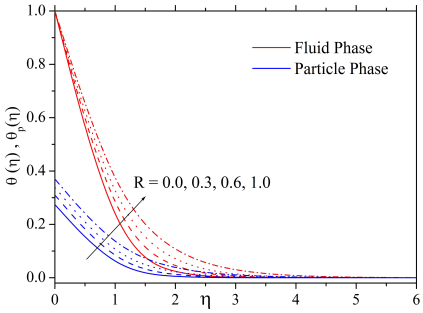

Figure 10: Influence of R on velocity profile.

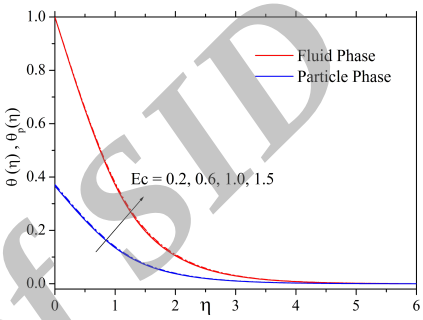

Figure 11: Influence of Ec on temperature profile.

by [[12], [32], [35]];

$$\begin{aligned} \rho c_p \left[u\frac{\partial T}{\partial x} + v\frac{\partial T}{\partial y} \right] \\ = k\frac{\partial^2 T}{\partial y^2} \\ + \frac{\rho_p c_m}{\tau_T}(T_p - T) \\ + \frac{\rho_p}{\tau_v}(u_p - u)^2 - \frac{\partial q_r}{\partial y}, \end{aligned} \tag{3.10}$$

$$\begin{aligned} \rho_p c_m \left[u_p\frac{\partial T_p}{\partial x} + v_p\frac{\partial T_p}{\partial y} \right] \\ = \frac{\rho_p c_m}{\tau_T}(T - T_p), \end{aligned} \tag{3.11}$$

where T and T_p are the temperature of the fluid and dust particles respectively, c_p and c_m are the specific heat of fluid and dust particles respectively, τ_T-the thermal equilibrium time i.e, the time required by the dust cloud to adjust its temperature to that of fluid, k-thermal conductivity of the fluid and and q_r-radiative heat flux.

The last three terms on the right side of (3.10) represent the heat conduction between the fluid and dust particles, energy generated to work done

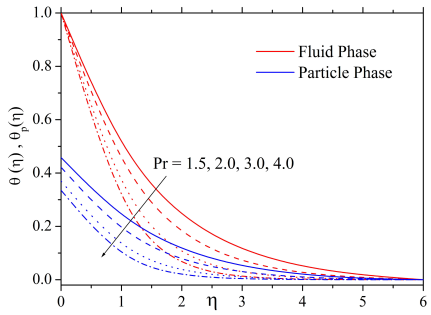

Figure 12: Influence of Pr on temperature profile.

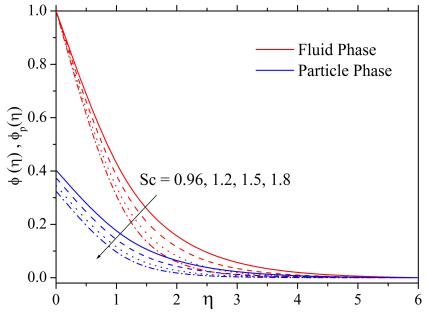

Figure 13: Influence of Sc on temperature profile.

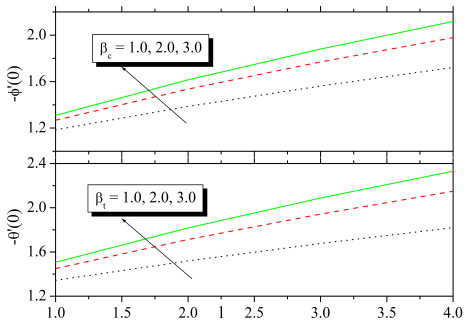

Figure 14: Variation of $-\theta'(0)$ and $-\phi'(0)$ for different values of β_t and β_c respectively.

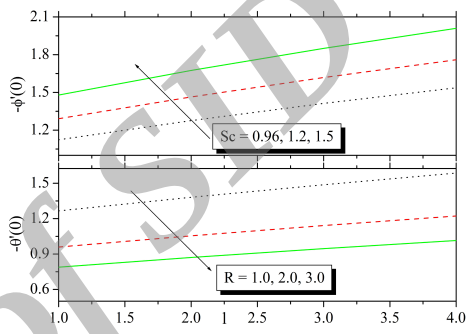

Figure 15: Variation of $-\theta'(0)$ and $-\phi'(0)$ for different values of R and Sc respectively.

by velocities and thermal radiation respectively. Now, according to the Rosseland diffusion approximation for radiation q_r is given by;

$$q_r = -\frac{4\sigma^*}{3k^+}\frac{\partial T^4}{\partial y}, \tag{3.12}$$

where σ^* is the Stefan-Boltzman constant and k^+-mean absorption coefficient. It is noted that the optically thick radiation limit is considered in this model. Assuming that the differences in the temperature within the flow are such that T^4 can be expressed as linear combination of the temperature, we expand T^4 in a Tayler series about T_∞ as follows

$$\begin{aligned} T^4 &= {T^4}_\infty + 4{T^3}_\infty(T - T_\infty) \\ &\quad +6{T^2}_\infty(T - T_\infty)^2 + \cdots, \end{aligned} \tag{3.13}$$

Neglect the higher order terms beyond the first degree in $(T - T_\infty)$,then one can get;

$$T^4 \cong 4{T^3}_\infty T - 3{T^4}_\infty, \tag{3.14}$$

Substituting equation (3.14) in equation (3.12) then one can get

$$\frac{\partial q_r}{\partial y} = -\frac{16T_\infty^4\sigma^*}{3k^+}\frac{\partial^2 T}{\partial y^2}. \tag{3.15}$$

In view of the equation (3.15), the energy equation (3.10) becomes

$$\begin{aligned} \rho c_p\left[u\frac{\partial T}{\partial x} + v\frac{\partial T}{\partial y}\right] &= (k + \frac{16T_\infty^4\sigma^*}{3k^+})\frac{\partial^2 T}{\partial y^2} \\ &\quad +\frac{\rho_p c_p}{\tau_T}(T_p - T) \\ &\quad +\frac{\rho_p}{\tau_v}(u_p - u)^2. \end{aligned} \tag{3.16}$$

Corresponding boundary conditions for the temperature are considered as follows;

$$\begin{aligned} T = T_w = bx + T_\infty \ \text{ at } \ y = 0, \\ T \longrightarrow T_\infty, \ \ T_p \longrightarrow T_\infty \ \text{ as } \ y \longrightarrow \infty \end{aligned} \tag{3.17}$$

where b is a positive constant.

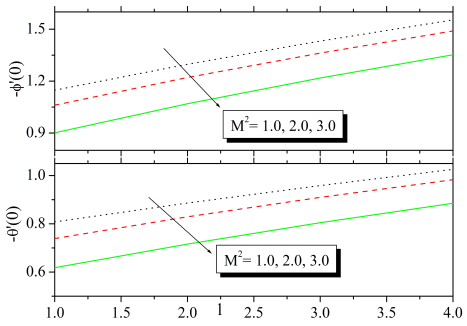

Figure 16: Variation of $-\theta'(0)$ and $-\phi'(0)$ for different values of M^2.

The dimensionless fluid phase temperature $\theta(\eta)$ and dust phase temperature $\theta_p(\eta)$ are defined as:

$$\theta(\eta) = \frac{T - T_\infty}{T_w - T_\infty}, \quad \theta_p(\eta) = \frac{T_p - T_\infty}{T_w - T_\infty}, \tag{3.18}$$

Using (3.18) into (3.16) and (3.11), we obtain the following non-linear ordinary differential equations:

$$\begin{aligned} &(1 + \frac{4}{3}R)\theta''(\eta) \\ &+Pr\left[\theta'(\eta)f(\eta) - \theta(\eta)f'(\eta)\right] \\ &+Prl\beta_t\gamma\left[\theta_p(\eta) - \theta(\eta)\right] \\ &+Pr\beta_v lEc\left[F'(\eta) - f'(\eta)\right]^2 = 0, \end{aligned} \tag{3.19}$$

$$\begin{aligned} &\theta_p'(\eta)F(\eta) - \theta_p(\eta)F'(\eta) \\ &-\beta_t\left[\theta_p(\eta) - \theta(\eta)\right] = 0, \end{aligned} \tag{3.20}$$

with

$$\begin{aligned} &\theta(\eta) = 1, \text{ at } \eta = 0, \\ &\theta(\eta) \longrightarrow 0, \ \theta_p(\eta) \longrightarrow 0, \\ &\text{as } \eta \longrightarrow \infty \end{aligned} \tag{3.21}$$

where $Pr = \frac{\mu c_p}{k}$ is the Prandtl number, $Ec = \frac{u_w^2}{c_p(T_w - T_\infty)}$ is the Eckret number, $\gamma = \frac{c_m}{c_p}$ is the specific heat ratio, $\beta_t = \frac{1}{b\tau_T}$ is fluid-particle interaction parameter for temperature and $R = \frac{4\sigma^* T_\infty^3}{k^+ k}$ is thermal radiative parameter.

Mass Transfer Analysis

The dust particles gain mass concentration from the fluid by diffusion through their spherical surface [32]. The conservation mass equations for both the fluid and dust phase are correspondingly given by;

$$\begin{aligned} \left[u\frac{\partial C}{\partial x} + v\frac{\partial C}{\partial y}\right] &= D_m\frac{\partial^2 C}{\partial y^2} \\ &+\frac{\rho_p}{\rho\tau_C}(C_p - C), \end{aligned} \tag{3.22}$$

$$\left[u_p\frac{\partial C_p}{\partial x} + v_p\frac{\partial C_p}{\partial y}\right] = \frac{1}{\tau_C}(C - C_p) \tag{3.23}$$

where C and C_p are concentration species of the fluid and particle phase, D_m is the mass diffusivity coefficient, τ_C is the time required by a dust particle to adjust its concentration relative to the fluid. The last term in the equation (3.22) represents the mass diffusion between the fluid and dust particles.

The relevant boundary conditions for the concentration fields are given by;

$$\begin{aligned} &C = C_w \text{ at } y = 0, \\ &C \to C_\infty, \ C_p \to C_\infty \text{ as } y \to \infty \end{aligned} \tag{3.24}$$

Now define the non-dimensional fluid phase concentration$\phi(\eta)$ and dust particle phase concentration $\phi_p(\eta)$ as

$$\phi(\eta) = \frac{C - C_\infty}{C_w - C_\infty}, \quad \phi_p(\eta) = \frac{C_p - C_\infty}{C_w - C_\infty} \tag{3.25}$$

Substituting (3.25) into (3.22) and (3.23), we obtain the following non-linear ordinary differential equations;

$$\begin{aligned} &\phi''(\eta) - Sc\left[f'(\eta)\phi(\eta) - f(\eta)\phi(\eta)\right] \\ &+Sc\beta_c l\left[\phi_p(\eta) - \phi(\eta)\right] = 0, \end{aligned} \tag{3.26}$$

$$\begin{aligned} &\phi_p'(\eta)F(\eta) - F'(\eta)\phi_p(\eta) \\ &+\beta_c\left[\phi(\eta) - \phi_p(\eta)\right] = 0, \end{aligned} \tag{3.27}$$

with

$$\begin{aligned} &\phi(\eta) = 1 \text{ at } \eta = 0, \\ &\phi(\eta) = 0, \ \phi_p(\eta) = 0 \text{ as } \eta \to \infty, \end{aligned} \tag{3.28}$$

where $Sc = \frac{\nu}{D_m}$ is the Schmidt number and $\beta_c = \frac{1}{b\tau_c}$ is fluid-particle interaction parameter for concentration.

The quantities of practical interest are the skin friction coefficient, local Nusselt number and local Sherwood number. Which are defined as;

$$\begin{aligned} &C_f = \frac{\tau_w}{\rho_f {U_w}^2}, \ Nu = \frac{xq_w}{k(T_w - T_\infty)}, \\ &Sh = \frac{xj_w}{D_m(C_w - C_\infty)}, \end{aligned} \tag{3.29}$$

where τ_w , q_w and j_w are the surface shear stress, heat flux and mass flux respectively and which are given by;

$$\tau_w = \mu \left(\frac{\partial u}{\partial y}\right)_{y=0}, \quad q_w = -k \left(\frac{\partial T}{\partial y}\right)_{y=0}, \quad j_w = -D_m \left(\frac{\partial C}{\partial y}\right)_{y=0}. \tag{3.30}$$

Using similarity transformations we get;

$$C_f {Re_x}^{1/2} = f''(0), \; Nu/{Re_x}^{1/2} = -\theta'(0), \; Sh/{Re_x}^{1/2} = -\phi'(0). \tag{3.31}$$

where $Re_x = \frac{u_w x}{\nu}$ is local Reynolds number.

4 Numerical Solution

The reduced set of similarity equations are coupled and non-linear in nature, thus it is very difficult to obtain closed form solutions. Therefore, we resorted to numerical solution by using Shooting method with fourth-fifth order Runge-Kutta-Fehlberg integration scheme. In Maple, the Shooting method is implemented in an algorithm referred as 'shoot'. This algorithm in Maple has been well tested for its accuracy and robustness and this has been used to solve a wide range of non-linear problems. More details about the 'shoot' algorithm can be found in Meade et al [25]. It is most important to choose the appropriate finite values of η_∞. It is most important to choose the appropriate finite values of η_∞. In this method, we choose suitable finite value of η_∞ as η_6 in accordance with standard practice in the boundary layer analysis. Further, for numerical computation the relative error tolerance to 10^-6 is considered for convergence and step size is chosen as $\triangle\eta = 0.001$.

In order to validate and verify the accuracy of the applied numerical scheme, results of $-\theta'(0)$ for various values of Pr with $M = l = R = 0$ are compared with those reported by Grubka and Bobba [18], Ishak et al [21] and El-Aziz [4]. The comparisons are shown in table 1 and it is witnessed that the solutions are in very good agreement for all the considered values of parameters.

5 Results and Discussion

A steady two dimensional boundary layer momentum, heat and mass transfer over a stretching sheet in the presence of thermal radiation and applied magnetic field is examined. The velocity, temperature and concentration profiles are depicted graphically for different physical parameters. For this objective figure 1-16 are plotted and numerical values for skin friction co-efficient, Nusselt number and Sherwood number are also presented.

The influence of magnetic parameter ($\mathbf{M^2}$):

The influence of magnetic parameter on fluid and dust particle phase velocity, temperature and concentration profiles are drawn in figures 1, 2 and 3 respectively. Figure 1 elucidates that, the velocity field and momentum boundary layer thickness reduces by an increasing magnetic parameter in both phases. Further, both temperature and concentration profile enhanced with magnetic parameter as shown in figures 2 and 3 correspondingly. Physically speaking, the magnetic field normal to an electrically-conducting fluid has the tendency to produce a drag-like force called the Lorentz force, which acts in the direction opposite to that of the flow, causing a flow retardation effect. Reduction in the velocity is responsible for thickening the thermal and solutal boundary layer thickness. The effect of magnetic parameter on $f''(0)$, $-\theta'(0)$ and $-\phi'(0)$ are also collected in the Table 2. It is observed that, the magnitude of skin friction, Nusselt number and Sherwood number are decreased by increase in magnetic parameter.

The influence of mass concentration dust particles parameter (l):

The effect of dust particles mass concentration on fluid and dust phase velocity, temperature and concentration profiles are demonstrated in the figure 4, 5 and 6 respectively. An introduction of dust particles in a clean fluid causes an internal friction within the fluid, which results retardation in fluid flow. Further, the dust particles absorb the heat from the fluid when they come into contact; this tends to reduce the temperature as well as the concentration of the fluid. This physical behaviour is clarified through the figures 4-6. That is, by increasing l, the velocity, temperature and concentration profiles of both the phase as well as their corresponding boundary layer thick-

ness will decreases. The skin friction co-efficient decreases and both Nusselt and Sherwood number increases with an increase in l as can be shown in Table 2.

The influence of fluid-particle interaction parameters ($\mathbf{fi_v}, \mathbf{fi_t}, \mathbf{fi_c}$):

The influence of fluid-particle interaction parameters $\beta_v, \beta_t, \beta_c$ on velocity, temperature and concentration profiles for both fluid and dust phase are captured in graphs 7-9. It is found that, if β_v, β_t and β_c are increased then the fluid phase velocity, temperature and concentration profiles get decreases. While the velocity, temperature and concentration profiles for dust phase are significantly increased. It is also evident from these plots that, for very large values of if β_v, β_t and β_c i.e., the relaxation time of the dust phase retards then the velocity, temperature and concentration profiles for both the phases will be same. The effect of if β_v, β_t and β_c on skin friction co-efficient, Nusselt number and Sherwood number is recorded in Table 2. The Table 2 depicts that, the skin friction co-efficient, Nusselt number and Sherwood number are decreasing function of β_v. But the Nusselt number and Sherwood number are increasing functions of β_t and β_c correspondingly.

The influence of thermal radiation parameter (R):

Figure 10 is plotted to notice the variation of thermal radiation parameter on the temperature profile for fluid and dust phase. This figure depicts that, the temperature profile as well as its corresponding boundary layer thickness is increased with thermal radiation parameter for both fluid and dust phase. Further, it depicts that, the thermal boundary layer thickness is higher in the presence of thermal radiation effect $(i.e., R \neq 0))$ than in the absence $(i.e., R = 0)$. Thus, in order to facilitate cooling process in industrial applications the radiation effect should be keep minimum. From Table 2 it is also observed that, the Nusselt number decreases with an increase in R.

The influence of Eckert number (Ec):

Figure 11 is sketched for both fluid and dust phase temperature distributions against Eckert number. By analysing this graph, we observed that the Eckert number significantly increases the temperature distribution in the flow region. The fact behind this mechanism is that the heat energy is stored in the fluid due to the frictional heating. The effect of increasing Ec enhances the temperature at any point and which is true for both fluid as well as dust phase. The Nusselt number enhanced notably with an increase in Ec.

The influence of Prandtl number (Pr):

Figure 12 refers to the variation of fluid and dust phase temperature distributions against Prandtl number. The temperature profile for both the phase is gradually decreased with an increase in Prandtl number. Also, it is seen from the Table 2 that, the Nusselt number increases with increase in Pr. This is because, a higher Prandtl number fluid has a relatively low thermal conductivity, which reduces conduction and as a result the thermal boundary layer thickness diminishes.

The influence of Schmidt number (Sc):

The concentration profiles for various values of the Schmidt number are presented in figure 13. This figure shows that, the concentration of both fluid and dust phase at the surface is smaller for larger value of Schmidt number. This outcome is expected, since the heat transfer analogue of the Schmidt number is the Prandtl number. Physically, Schmidt number is a ratio of momentum diffusivity and mass diffusivity. Mass diffusivity increases with an increase in Schmidt number, consequently solutal boundary layer thickness decreases. The expected outcome is seen in Table 2 that, the Sherwood number is an increasing function of the Schmidt number.

The influence of Nusselt and Sherwood numbers:

Figure 14 illustrates the variation of the Nusselt number $-\theta'(0)$ and Sherwood number $-\phi'(0)$ versus mass concentration of dust particles l for various values of the β_t and β_c respectively. It is observed that, both Nusselt number and Sherwood number enhanced by increasing the values of β_t and β_c correspondingly. Figure 15 is plotted to depict the effects of R and Sc on Nusselt number and Sherwood number against l. This figure elucidates that, the Nusselt number decreases for increasing values of R and the Sherwood number increases by strengthening the Schmidt number. The response of Nusselt and Sherwood number in opposition to l for different values of magnetic parameter is presented in figure 16. From this figure, one can notice that the effect of magnetic field reduces the Nusselt and Sherwood numbers.

That is, both Nusselt and Sherwood number profiles are decreasing functions of magnetic parameter. Further, both the Nusselt and Sherwood numbers significantly increases with mass concentration of dust particles. From this one can conclude that, the dusty fluid has higher Nusselt and Sherwood numbers than ordinary fluid. It is hoped that, the dusty fluids are more preferable for industrial applications in liquid-particle based systems involving high rate of heat transfer.

6 Conclusion

Theoretical analysis of hydromagnetic boundary layer flow, heat and mass transfer of a dusty fluid over a stretching sheet has been investigated numerically. The important conclusions are summarized as follows.

An increase in the magnetic parameter has the effect of thickening the temperature and concentration profiles, while it has an inhibiting effect on the velocity field. The momentum and thermal boundary layer are thinner due to the influence of suspended dust particles. The effect of Prandtl number is to decrease the thermal boundary layer thickness. The effect of Schmidt number is to decrease the fluid and particle phase concentration profiles, whereas the concentration of the fluid phase decreases and dust phase increases with an increase in fluid-particle interaction parameter for concentration. An increase in the Schmidt number results in suppressing the concentration distribution. The Nusselt number is an increasing function of β_t, whereas this trend is quite opposite for M^2 and R. Further, it is observed that the Sherwood number enhances with increasing the values of β_c and Sc, but an opposite result is obtained for larger values of M^2.

Acknowledgement

We are grateful to reviewers for the useful suggestions. Further, one of the authors (B. J. Gireesha) is thankful to the University Grants Commission, India, for the financial support under the scheme of Raman Fellowship for Post-Doctoral Research for Indian Scholars in USA.

References

[1] V. M. Agranat, *The effect of pressure gradient on friction and heat transfer in a dusty boundary layer*, Fluid Dynamics (Springer) 23 (1988) 729-732.

[2] M. E. Ali, F. Al-Youself, *Laminar mixed convection from a continuously moving vertical surface with suction or injection*, Heat Mass Transfer 33 (1998) 301-306.

[3] H. A. Attia, W. Abbas, M. A. Abdeen, M. S. Emam, *Effect of porosity on the flow of a dusty fluid between parallel plates with heat transfer and uniform suction and injection*, Eur J Environ Civil Eng 18 (2014) 241-251.

[4] M. A. Aziz, *Mixed convection flow of a micropolar fluid from an unsteady stretching surface with viscous dissipation*, Journal of the Egyptian Mathematical Society 21 (2013) 385-394.

[5] K. J. Basant, C. A. Apere, *Unsteady MHD two-phase Couette flow of fluid-particle suspension*, Applied Mathematical Modelling 37 (4) (2012) http://dx.doi.org/10.1063/1.3657509/.

[6] A. Bejan, K. R. Khair, *Heat and mass transfer by natural convection in a porous medium*, Int. J. Heat Mass Transfer 28 (1985) 909-918.

[7] A. J. Chamkha, A. K. Abdul-Rahim, *Similarity solutions for hydromagnetic mixed convection heat and mass transfer for Hiemenz flow through porous media*, International Journal of Numerical Methods for Heat and Fluid Flow 10 (2000) 94-115.

[8] A. J. Chamkha, A. K. Abdul-Rahim, *Hydromagnetic combined heat and mass transfer by natural convection from a permeable surface embedded in a fluid-saturated porous medium*, International Journal of Numerical Methods for Heat and Fluid Flow 10 (2000) 455 - 477.

[9] A. J. Chamka, *Particulate viscous effects on the compressible boundary-layer two-phase flow over a flat plate*, Int Comm Heat Mass Transfer 25 (1998) 279-288.

[10] N. Datta, S. K. Mishra, *Boundary layer flow of a dusty fluid over a semi infinite flat plate*, Acta Mechanica 42 (1982) 71-83.

[11] B. J. Gireesha, B. Mahanthesh, M. M. Rashidi, *MHD boundary layer heat and mass transfer of a chemically reacting Casson fluid over a permeable stretching surface with non-uniform heat source/sink*, Int. J. Industrial Mathematics 7 (2015) 247-260.

[12] B. J. Gireesha, B. Mahanthesh, I. S. Shivakumara, K. M. Eshwarappa , *Melting heat transfer in boundary layer stagnation-point flow of nanofluid toward a stretching sheet with induced magnetic field*, http://dx.doi.org/10.1016/j.jestch.2015.07.012/.

[13] B. J. Gireesha, G. S. Roopa, C. S. Bagewadi, *Effect of viscous dissipation and heat source on flow and heat transfer of dusty fluid over unsteady stretching sheet*, Appl Math Mech 33 (2012) 1001-1014.

[14] B. J. Gireesha, A. J. Chamkha, C. S. Vishalakshi, C. S. Bagewadi, *Three-dimensional Couette flow of a dusty fluid with heat transfer*, Applied Mathematical Modelling 36 (2012) 683-701.

[15] B. J. Gireesha, B. Mahanthesh, R. S. R. Gorla, *Suspended particle effect on nanofluid boundary layer flow past a stretching surface*, Journal of Nanofluids 3 (2014) 267-277.

[16] B. J. Gireesha, B. Mahanthesh, R. S. R. Gorla, P. T. Manjunatha, *Thermal radiation and Hall effects on boundary layer flow past a non-isothermal stretching surface embedded in porous medium with non-uniform heat source/sink and fluid-particle suspension*, Heat Mass Transfer http://dx.doi.org/10.1007/s00231-015-1606-3/.

[17] B. J. Gireesha, K. L. Krupa Lakshmi, B. Mahanthesh, R. S. R. Gorla, *Effects of diffusion-thermo and thermo-diffusion on two-phase boundary layer flow past a stretching sheet with fluid-particle suspension and chemical reaction: A numerical study*, Journal of the Nigerian Mathematical Society http://dx.doi.org/10.1016/j.jnnms.2015.10.003/.

[18] L. J. Grubka, K. M. Bobba, *Heat transfer characteristics of a continuous stretching surface with variable temperature*, ASME J Heat Transfer 107 (1985) 248-250.

[19] A. M. Guzman, C. H. Amon, *Convective Heat Transfer and Flow Mixing in Converging-Diverging Channel Flows*, Heat Transfer Division 361 (1998) 61-68.

[20] F. M. Hady, R. S. R. Gorla, *Heat transfer from a continuous surface in a parallel free stream of viscoelastic fluid*, Acta Mechanica 128 (1998) 201-208.

[21] A. Ishak, R. Nazar, I. Pop, *Boundary layer flow and heat transfer over an unsteady stretching vertical surface*, Meccanica 44 (2009) 369-375.

[22] F. C. Lai, F. A. Kulacki, *Coupled heat and mass transfer from a sphere buried in an infinite porous medium*, Int. J. Heat Mass Transfer 33 (1990) 209-215.

[23] E. Magyari, M. E. Ali, B. Keller, *Heat and mass transfer characteristics of the self similar boundary layer flows induced by continuous surface stretched with rapidly decreasing velocities*, Heat Mass Transfer 38 (1998) 65-74.

[24] O. D. Makinde, T. Chinyoka, *MHD transient flows and heat transfer of dusty fluid in a channel with variable physical properties and Navies slip condition*, Compu Math Appl 60 (2010) 660-669.

[25] D. B. Meade, B. S. Haran, R. E. White, *The shooting technique for the solution of two-point boundary value problems*, Maple Technologies 3 (1996) 85-93.

[26] M. Muhaimin, R. Kandasamy, A. B. Khamis, *Effects of heat and mass transfer on nonlinear MHD boundary layer flow over a shrinking sheet in the presence of suction*, Appl. Math. Mech. 29 (2008) 1309-1317.

[27] D. Pal, *Combined effects of non-uniform heat source/sink and thermal radiation on heat transfer over an unsteady stretching permeable surface*, Comm in Nonlin. Sci. Numer. Simu. 16 (2011) 1890-1904.

[28] G. Palani, P. Ganesan, *Heat transfer effects on dusty gas flow past a semi-infinite inclined plate*, Forsch Ingenieurwes (Springer) 71 (2007) 223-230.

[29] M. T. Ray, A. S. Gupta, *Heat transfer in stagnation-point flow towards a stretching sheet*, Heat Mass Transfer 38 (2002) 517-521.

[30] M. M. Rashidi, A. Hosseini, I. Pop, S. Kumar, N. Freidoonimehr, *Comparative numerical study of single and two-phase models of nanofluid heat transfer in wavy channel*, Applied Mathematics and Mechanics 35 (2014) 831-848.

[31] M. M. Rashidi, A. B. Parsa, S. Abelman, *MHD natural convection with convective surface boundary condition over a flat plate*, Abstract and Applied Analysis, Article ID 923487 10 pages.

[32] P. G. Saffman, *On the stability of laminar flow of a dusty gas*, J. Fluid Mechanics 13 (1962) 120-128.

[33] B. C. Sakiadis , *Boundary layer behaviour on continuous solid surface*, AIChE J. 7 (1961) 26-28.

[34] F. K. Tsou, E. M. Sparrow, R. J. Goldstein, *Flow and heat transfer in the boundary layer on a continuous moving surface*, Int J Heat Mass Transfer 10 (1967) 219-235.

[35] R. Tiwari, K. Singh, *Effect of hall current on unsteady hydromagnetic boundary layer in rotating dusty fluid*, Ind J of Pure and Applied Math 14 (1982) 159-165.

[36] R. Tsai, J. S. Huang, *Heat and mass transfer for Soret and Dufours effects on Hiemenz flow through porous medium onto a stretching surface*, Int. J. Heat and Mass Transfer 52 (2008) 2399-2406.

[37] K. Vajravelu, J. Nayfeh, *Hydromagnetic flow of a dusty fluid over a stretching sheet*, International Journal of linear Mech 27 (1992) 937-945.

Koneri Lakshmikanthraj Krupa Lakshmi is born in Holenarasipura Karnataka, INDIA in 1983.she received her M.Sc in Mysore University, Mysore, India and M.phil in Vinayaka Missions University, Salem, India. She joined as a research scholar in the Department of Mathematics, Kuvempu University in 2012 and she is continuing research till now. Her research interests are Boundary layer flow, heat and mass transfer and dusty fluid flow problems.

Bijjanal Jayanna Gireesha is a Assistant Professor in Department of Mathematics at Kuvempu University, Karnataka and received M.Phil (1999) and Ph.D (2002) in Fluid Mechanics from Kuvempu University, Shimoga, India. Currently he is working as a visiting research faculty in Department of Mechanical Engineering Cleveland State University, Cleveland, USA. His research interests include the areas of Fluid mechanics particularly, boundary layer flows, Newtonian/ non-Newtonian fluids, heat and mass transfer, Nanofluid flow problems.

Dr. Rama S.R. Gorla is Fenn Distinguished Research Professor in the Department of Mechanical Engineering at Cleveland State University. He received the Ph.D. degree in Mechanical Engineering from the University of Toledo in 1972. His primary research areas are combustion, heat transfer and fluid dynamics. He has been recently involved in the testing and development of a three-dimensional Navier Stokes Computational Code for Wright Patterson Air Force Base. He worked as a turbomachinery design engineer at Teledyne Continental Motors Turbine Engines (TCM-TE) in Toledo, Ohio and as a design engineer of the aerothermodynamics of rotating machinery at Chrysler Corporation in Highland Park, Michigan. He completed a research program funded by NASA Lewis Research Center in Turbine Heat Transfer. Dr. Gorla has published over 350 technical papers in refereed jour-

nals and contributed several book chapters in Encyclopedia of Fluid Mechanics. NASA, AFOSR and local industry have sponsored his research. He co-authored a text book on Turbomachinery published by Marcel Dekker Company in 2003. He is the Editor-in-Chief of the International Journal of Fluid Mechanics Research and Associate Editor of five Journals: International Journal of Turbo and Jet Engines, Applied Mechanics and Engineering Journal, Journal of MHD and Plasma Research, Journal of Mechanics of Continua and Mathematical Sciences and the Journal of Pure and Applied Physics.

Basavarajappa Mahanthesh is Assistant Professor in the Department of Mathematics and Statistics, CHRIST UNIVERSITY, Bangalore, India. Further, he is a Research scholar at Department of Mathematics, Kuvempu University, Shimoga. His research interests cover the three-dimensional boundary layer flows, fluid-particle suspension, nanofluid and Heat/Mass transfer.

Two-phase Boundary Layer Flow, Heat and Mass Transfer of a Dusty Liquid past a Stretching Sheet with Thermal Radiation

K. L. Krupa Lakshmi, B. J. Gireesha, Rama S R Gorla, B. Mahanthesh

انعطاف‌پذیری تغییرات در مدل‌های شعاعی و غیرشعاعی تحلیل پوششی داده‌ها

چکیده:

یکی از مسایل اصلی در تحلیل پوششی داده‌ها عبارت است از تعیین تصویر واحدهای تصمیم‌گیرنده ناکارا بر مرز کارایی. در مدل‌های متداول تحلیل پوششی داده‌ها، ورودی و خروجی‌های واحدهای تصمیم گیرنده ناکارا به منظور رسیدن به مرز کارایی به اندازه دلخواه تغییر می‌کنند. با این وجود توانایی واحدهای تصمیم‌گیرنده گاهی اوقات تعریف و مقید می‌شود. به علاوه در برخی موقعیت‌ها ازکاربردهای واقعی منابع محدود وجود دارند. بنابراین در این موارد ورودی و خروجی‌ها نمی‌توانند به طور نامعقول تغییر کنند. در حقیقت سطوح تغییر از پیش تعیین‌شده‌ای از ورودی و خروجی‌ها وجود دارند. بدین منظور برای ارزیابی کارایی نسبی واحدها با حضور متغیرهای ورودی و خروجی مقید، مدل‌های شعاعی و غیر شعاعی مبتنی بر تحلیل پوششی داده‌ها در بررسی حاضر ارایه می‌شود. علاوه بر این مدل‌های ابرکارایی غیرشعاعی به منظور رتبه‌بندی واحدهای تصمیم‌گیرنده کارا بسط می‌یابند. یک مثال از بخش بانکداری به منظور توضیح روش پیشنهادی به کار می‌رود.